Research Article | Vol. 29, No. 21 / 11 Oct 2021 / Optics Express 33491
Optics EXPRESS

Low jitter microwave pulse train generation based on an optoelectronic oscillator

ZIWEN HE,[1] LINGZHI LI,[1] JIEJUN ZHANG,[1,*] AND JIANPING YAO[2]

[1]Guangdong Provincial Key Laboratory of Optical Fiber Sensing and Communications, Institute of Photonics Technology, Jinan University, Guangzhou 511443, China
[2]Microwave Photonics Research Laboratory, School of Electrical Engineering and Computer Science, University of Ottawa, Ottawa, ON K1N 6N5, Canada
*zhangjiejun@jnu.edu.cn

Abstract: We demonstrate an approach to ultra-short pulse train generation with a low time jitter based on pulse compression of a frequency comb generated by a dual-loop optoelectronic oscillator (OEO). The proposed dual-loop OEO consists of two feedback loops, with one having a long loop length and the other a short loop length. In the long loop, a phase modulator (PM) cascaded with a Mach-Zehnder modulator (MZM) are employed, and in the short loop, only the MZM is included. Due to the Vernier effect, the use of the dual-loop structure can facilitate mode selection to generate a single-frequency microwave carrier with multiple optical sidebands corresponding to an optical comb. By adjusting the phase relationship between the optical sidebands using a dispersion compensating fiber (DCF), a stable optical pulse train is generated. Thanks to the low phase noise nature of an OEO, the generated pulse train has a low time jitter. The proposed approach is evaluated experimentally. A pulse train with a repetition frequency of 2.023 GHz and a pulse width of 40 ps is generated. The single-sideband (SSB) phase noise of the carrier frequency generated by the OEO is measured to be −118 dBc/Hz at a 10-kHz offset frequency, corresponding to a time jitter of the pulse train of 391.2 fs. The phase noise can be further reduced if an active cavity stabilization mechanism is adopted, enabling further reduction in the time jitter to the order of tens of femtoseconds.

1. Introduction

An ultra-short pulse train with a low time jitter can find a variety of applications, such as high-speed communications, high precision spectroscopy, millimeter-wave and terahertz waveform generation, and radar systems [1,2]. In those applications, time jitter is one of the most critical parameters, which has a strong influence on the overall system performance. For example, in a time-of-flight (TOF) measurement system, the accuracy of the displacement measurement is highly dependent on the time jitter [3]. In a communication system, low time jitter is required in the clock recovery process to ensure high-speed transmission [4]. Due to the high repetition rate and low time jitter, pulse train generation based on photonics has been well studied and numerous techniques have been proposed and demonstrated.

Fiber-based mode locking has been demonstrated to be an effective approach to generating an optical pulse train with a low time jitter [5]. A coupled opto-electronic oscillator (COEO) consisting of a mode-locked laser (MLL) and an optoelectronic oscillator (OEO) was also demonstrated to generate a microwave pulse train with low timing jitter [6,7]. However, a fiber-based MLL source or an COEO is usually complicated and costly due to the need for high-precision dispersion management and stable phase locking to ensure a stable operation. In addition, the repetition frequency of an MLL pulse train is either fixed in a passively MLL source, or discretely tunable in an actively MLL source [8]. In [9], an OEO based on injection locking between two laser diodes was demonstrated to generate an optical pulse train with 20-ps

#440257 https://doi.org/10.1364/OE.440257
Journal © 2021 Received 11 Aug 2021; revised 20 Sep 2021; accepted 22 Sep 2021; published 29 Sep 2021

Optics EXPRESS

pulse width. However, stable phase locking between laser diodes may be difficult to maintain, and the system can only generate a small number of comb lines. To generate a pulse train with continuously tunable repetition rate, optical modulation may be employed [10–18]. For example, in [10] a continuous-wave (CW) light from a narrow-linewidth laser source was phase modulated to a deeply chirped light, which was then compressed by a dispersive component to generate a short pulse with a sub-picosecond temporal width. However, to generate an optical comb with a large number of comb lines, a high modulation depth was needed, which requires that the microwave source has a high power, and the phase modulator has a low half-wave voltage. Cascading [11,12] or paralleling [13] two or more optical modulators can generate an optical comb with more comb lines, but the system is more complicated and the loss is high. Optical nonlinearity can be used to broaden the spectral width of an optical comb and further reduce the pulse width [14–17]. The amplitude and phase of the comb lines of an optical comb obtained through optical modulation can be engineered to generate an optical pulse with improved quality [14]. Although optical pulse train generation based on optical modulation does not require mode locking as compared with pulse train generation using an MLL source, an external microwave source is needed to drive the modulators, and the performance of the generated pulse train is highly dependent on the quality of the external microwave source. An OEO has been proven to be able to generate a microwave signal with low phase noise and wide frequency tunable range [19–22], thus can be used as a high-quality microwave source in a modulator-based pulse train generation system.

In this paper, we propose and experimentally demonstrate a microwave pulse train generation system based on a dual-loop OEO incorporating two electro-optic modulators. The OEO consists of two feedback loops, with one having a long loop length and the other a short loop length. In the long loop, a phase modulator (PM) cascaded with a Mach-Zehnder modulator (MZM) are employed, and in the short loop, only the MZM is included. Due to the Vernier effect, mode selection to enable single-frequency oscillation is ensured. The microwave carrier is modulated at the two modulators to generate multiple optical comb lines. The phase relationship in the comb lines is studied and it is found that the comb has a quadratic phase function, which can be changed to a linear phase function by using a dispersive element with linear dispersion. Thus, a pulse train with pulse compression is generated [23]. The proposed approach is experimentally demonstrated. A microwave carrier at 2.023 GHz is generated, which is modulated to generate an optical comb with over 10 comb lines. By using a dispersion compensating fiber (DCF) with a dispersion coefficient of −995.6 ps/nm as the dispersive element, the quadratic phase function of the optical comb is converted to a linear phase function and pulse compression is achieved. An optical pulse train with a repetition rate of 2.023 GHz and a pulse width of 40 ps is generated. The single-sideband (SSB) phase noise of the oscillation frequency is measured to be −118 dBc/Hz at a 10-kHz offset frequency, corresponding to a time jitter of 391.2 fs. If an active stabilization mechanism is employed, the phase noise at low offset frequency can be reduced and the time jitter can be further reduced with a few tens of fs [21,24–27].

2. Principle

2.1. System setup

Figure 1 shows the schematic diagram of the proposed microwave pulse train generator. A laser diode (LD) is used to generate a CW optical carrier, which is sent to a PM via a polarization controller (PC1). By tuning PC1, the polarization direction of the optical carrier is aligned to the principal axis of the PM, to minimize the polarization-dependent insertion loss. In order to obtain an optical comb with an increased number of comb lines, we use two cascaded modulators (a PM and an MZM) to generate an optical comb with multiple comb lines. A single-mode fiber (SMF1) and a variable optical delay line (ODL) are incorporated in the OEO between the PM and the MZM, to introduce a time delay, to ensure a phase match between the

Optics EXPRESS

microwave signals applied to the PM and the MZM so that the modulation sidebands can have a determined phase relationship. A second PC (PC2) is used before the PM to minimize again the polarization-dependent loss. The optical signal at the output of the MZM, after passing through a second SMF (SMF2) and amplified by an erbium-doped fiber amplifier (EDFA), is split into two equal portions. One half of the optical signal is launched into a DCF where pulse compression is performed. A second half of the optical signal is sent to a second PD (PD2). The signal at the output of PD2, after passing through an electrical bandpass filter (EBPF) and amplified by an electronic amplifier (EA1), is split into two by a microwave power divider to drive the PM and the MZM. To maximize the power and number of the modulation sideband, the driving signal to the PM is frequency doubled by a frequency multiplier and further amplified by second EA (EA2). The operation of the OEO is monitored in the spectral domain by an electrical spectrum analyzer (ESA) an optical spectrum analyzer (OSA), and in the time domain by an oscilloscope (OSC).

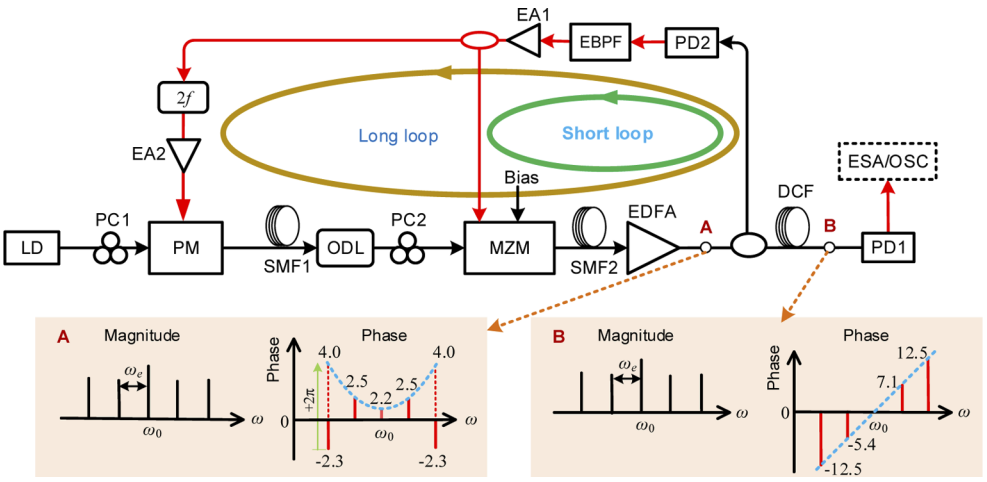

Fig. 1. Schematic diagram of the proposed pulse train generation system based on a dual-loop OEO. LD: laser diode; PC: polarization controller; PM: phase modulator; MZM: Mach-Zehnder modulator; EDFA: erbium-doped fiber amplifier; OC: optical coupler; PD: photodetector; EA: electric amplifier; ODL: optical delay line; SMF: single-mode fiber; DCF: dispersion compensating fiber; OSC: oscilloscope; OSA: optical spectrum analyzer; ESA: electricity spectrum analyzer.

2.2. OEO operation

By applying the microwave signal from PD2 to the PM and the MZM, the dual loops of the OEO are closed. Once the gain is higher than the loss, the OEO will start to oscillate. Assuming that the OEO oscillates at a fundamental frequency of ω_e, the microwave signals applied to the PM and MZM can be written as $E_{\mathrm{RF1}}(t) = V_1 \cos(2\omega_e t)$ and $E_{\mathrm{RF2}}(t) = V_2 \cos(\omega_e t)$, where V_1 and V_2 are the amplitudes of the microwave signals. The electric field of the optical signal at the output of the PM can be expressed as

$$E_{\mathrm{PM}}(t) = E_0 e^{j\left[\omega_0 t + \pi \frac{V_1}{V_\pi} \cos(2\omega_e t)\right]} \tag{1}$$

Optics EXPRESS

where E_0 is the amplitude of the electric field of the incident light wave, and V_π is the half-wave of the PM. Based on the Jacobi-Anger expansion, Eq. (1) can be rewritten as

$$\begin{aligned} E_{\mathrm{PM}} &= E_0 e^{j\omega_0 t} \sum_{n=-\infty}^{n=\infty} J_n(\xi) e^{j2n\omega_e t} \\ &\approx E_0 e^{j\omega_0 t}[J_0(\xi) + J_1(\xi) e^{j(2\omega_e t+\pi/2)} - J_{-1}(\xi) e^{j(-2\omega_e t-\pi/2)}] \\ &\approx E_0 e^{j\omega_0 t}[J_0(\xi) + J_1(\xi) e^{j2\omega_e t} + J_{-1}(\xi) e^{-j2\omega_e t}] \end{aligned} \tag{2}$$

where ω_0 is the angular frequency of the optical carrier, $J_n = J_n(\xi)$ is the n-th order Bessel function of the first kind, and $\xi = \pi V_1/V_\pi$ is the modulation depth of the PM. The higher-order sidebands are ignored in Eq. (2). Then, the phase modulated signal is intensity-modulated at the MZM. The electric field of the optical signal at the output of the MZM can be written as

$$\begin{aligned} E_{\mathrm{MZM}} &= \frac{1}{2} E_0 e^{j(\omega_0 t)} \sum_{n=-\infty}^{n=\infty} J_n(\xi) e^{j(2n\omega_e t+2n\omega\tau_1)} [e^{j(m\cos(\omega_e t)+\varphi_1)} + e^{-jm\cos(\omega_e t)}] \\ &= \frac{1}{2} E_0 e^{j(\omega_0 t)} \sum_{n=-\infty}^{n=\infty} J_n(\xi) e^{j(2n\omega_e t+2n\omega_e\tau_1)} e^{j(\varphi_1/2)} [\cos(m\cos(\omega_e t) + \varphi_1/2)] \\ &= \frac{1}{2} E_0 e^{j(\omega_0 t+\varphi_1/2)} \sum_{n=-\infty}^{n=\infty} J_n(\xi) e^{j(2n\omega_e t+2n\omega_e\tau_1)} \\ &\times [\cos(\varphi_1/2)\cos(m\cos(\omega_e t)) - \sin(\varphi_1/2)\sin(m\cos(\omega_e t))] \end{aligned} \tag{3}$$

Again, by applying the Jacobi-Anger expansion, Eq. (3) becomes

$$\begin{aligned} E_{\mathrm{MZM}} = \frac{1}{2} E_0 e^{j(\omega_0 t+\varphi_1/2)} & \\ \times \{ & \cos(\varphi_1/2) J_0(m) J_0(\xi) \\ & + \sin(\varphi_1/2) J_1(m) e^{-j\omega_e t} [J_0(\xi) + J_1(\xi) e^{-j2\omega\tau_1}] \\ & + \sin(\varphi_1/2) J_1(m) e^{j\omega_e t} [J_0(\xi) e^{-j\pi} + J_1(\xi) e^{j2\omega\tau_1}] \\ & + \cos(\varphi_1/2) J_0(m) J_1(\xi) e^{j(2\omega_e(t+\tau_1))} + \sin(\varphi_1/2) J_1(m) J_1(\xi) e^{j(\omega_e(3t+2\tau_1)+\pi)} \\ & + \cos(\varphi_1/2) J_0(m) J_1(\xi) e^{-j(2\omega_e(t+\tau_1)-\pi)} + \sin(\varphi_1/2) J_1(m) J_1(\xi) e^{-j(\omega_e(3t+2\tau_1)-\pi)} \} \end{aligned} \tag{4}$$

where φ_1 is a phase caused by the MZM bias voltage, $m = \pi V_2/V_\pi$ is the modulation depth of the MZM, τ_1 is the time delay between the PM and the MZM. According to Eq. (4), a frequency comb is generated at the output of the MZM and the comb lines are the sidebands generated due to the phase and intensity modulations. When the comb lines have a linear phase relationship, a transform-limited pulse train with a pulse width determined by the bandwidth of the frequency comb is generated.

The performance of the pulse generator relies on the quality of the microwave signal applied to the PM and the MZM. Here, the microwave signal is generated by an OEO, in which single-frequency selection is achieved by the dual loops with the assistance of a narrowband EBPF [19,20]. Thanks to the dual loops, the effective FSR is increased, which makes the selection of a single frequency much easier using an EBPF [17]. As shown in Fig. 1, the dual loops share a common path from the output of the MZM to the output of EA1. The signal at the output of EA1 is split into two parts, with one applied to the MZM and the other, after frequency doubling and electronic amplification, to the PM. Between the PM and the MZM, there is an ODL, which is tuned to achieve phase matching between the microwave signals applied to the PM and the MZM.

Optics EXPRESS

The modes supported by the dual loops should satisfy [19],

$$k_1/(\tau_1 + \tau_2) = k_2/\tau_2 \tag{5}$$

where k_1 and k_2 are integers and $\tau_1 = L_1 n_0/c$ and $\tau_2 = L_2 n_0/c$ are the time delays mainly contributed by SMF1 and SMF2, where L_1 and L_2 are the lengths of SMF1 and SMF2, respectively, n_0 is the refractive index, and c is the speed of light in vacuum.

In a dual-loop OEO, the mode spacing is determined by the short loop given by $\Delta f \approx 1/\tau_2$, and the phase noise is determined by the long loop. Thus, the use of dual loops have two major benefits: large mode spacing and low phase noise [19]. The mode spacing is determined by the short loop, while the overall Q factor is improved by the long loop, leading to a lower phase noise than that when only a short loop is used [28]. Figure 2 illustrates the mode selection in a dual-loop OEO, where FSR1, FSR2 and FSR3 are, respectively, the FSRs of the long, short, and dual loops.

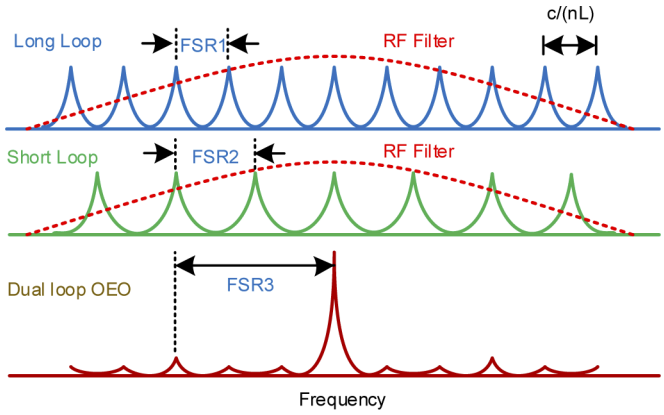

Fig. 2. Illustration of mode selection in a dual-loop OEO. Due to the Vernier effect, the FSR of the dual loops is increased which would facilitate mode selection for single-frequency oscillation of the OEO.

As pointed out, the phase noise of the dual loop OEO is determined by the long loop, and the mode interval is determined by the short loop. The phase noise is given by [20]

$$S(f') = \frac{\delta}{(\delta/2\tau) + (2\pi)^2(\tau f')^2} \tag{6}$$

where f' is the frequency offset from the oscillation frequency, $\tau \simeq \tau_1 + \tau_2$ is the time delay of the long loop jointly contributed by SMF1 and SMF2, and δ is a noise factor given by $\delta = \rho_N G_A^2/P_{\mathrm{OSC}}$, where G_A is the voltage gain, ρ_N and P_{OSC} are the noise power density and microwave power at the output of the PD (PD2), respectively. The time jitter of the pulse train, which is ultimately determined by the phase noise of the microwave carrier generated by the OEO [29], can be calculated by [25]

$$\delta_t = \sqrt{2P_N}/\omega \tag{7}$$

where P_N is the total phase noise power, which is calculated by

$$P_N = \int_0^{+\infty} S(f')df' \tag{8}$$

Optics EXPRESS

2.3. Pulse generation

To generate a microwave pulse train based on optical modulation, the comb lines must have a linear phase relationship [10,14]. For the proposed dual-loop OEO based on cascaded PM and MZM, the phase function of the optical comb has a nonlinear phase relationship. Direct detection of the comb lines at a PD will not generate a compressed pulse train. Based on Eq. (4), we can find that the phase relationship is approximately quadratic which can be compensated using a DCF [18]. The frequency response of a DCF is given by [30]

$$H_{\mathrm{DCF}}(\omega) = e^{j(\omega^2 \beta L/2)} \tag{9}$$

where ω is the optical frequency, β and L are the second-order dispersion and the length of the DCF, respectively. After propagating through the DCF, each of the comb lines at $\omega_0 + n \cdot \omega_e$ is multiplied by a phase term given by Eq. (9). As a result, the optical field at the output of the DCF can be calculated by

$$\begin{aligned} E_{\mathrm{DCF}} = & \frac{1}{2} E_0 e^{j(\omega_0 t + \varphi_1/2)} \\ & \times \{\cos(\varphi_1/2) J_0(m) J_0(\xi) \\ & + \sin(\varphi_1/2) J_1(m) e^{-j\omega_e t} [J_0(\xi) + J_1(\xi) e^{-j2\omega\tau_1}] e^{j(\omega_e{}^2 \beta L/2)} \\ & + \sin(\varphi_1/2) J_1(m) e^{j\omega_e t} [J_0(\xi) e^{-j\pi} + J_1(\xi) e^{j2\omega\tau_1}] e^{j(\omega_e{}^2 \beta L/2)} \\ & + \cos(\varphi_1/2) J_0(m) J_1(\xi) e^{j2\omega_e t} e^{j(2\omega_e \tau_1)} e^{j(2\omega_e)^2 \beta L/2)} \\ & + \cos(\varphi_1/2) J_0(m) J_1(\xi) e^{-j2\omega_e t} e^{-j(2\omega_e \tau_1 - \pi)} e^{j((2\omega_e)^2 \beta L/2)} \\ & + \sin(\varphi_1/2) J_1(m) J_1(\xi) e^{j3\omega_e t} e^{j(2\omega_e \tau_1 + \pi)} e^{j((3\omega_e)^2 \beta L/2)} \\ & + \sin(\varphi_1/2) J_1(m) J_1(\xi) e^{-j(3\omega_e t)} e^{-j(2\omega_e \tau_1 - \pi)} e^{j((3\omega_e)^2 \beta L/2)} \} \end{aligned} \tag{10}$$

Based on Eq. (10), the phase function of an optical comb generated based on the proposed dual-loop OEO is calculated. In the calculation, we assume the microwave signal generated by the dual-loop OEO has a frequency of 2 GHz. Figure 3(a) shows the phase function of the comb lines as the solid blue lines. As can be seen, the phase function is not linear. Thus, the detection of the comb lines at a PD will not generate a compressed pulse train. If we unwrap the phase

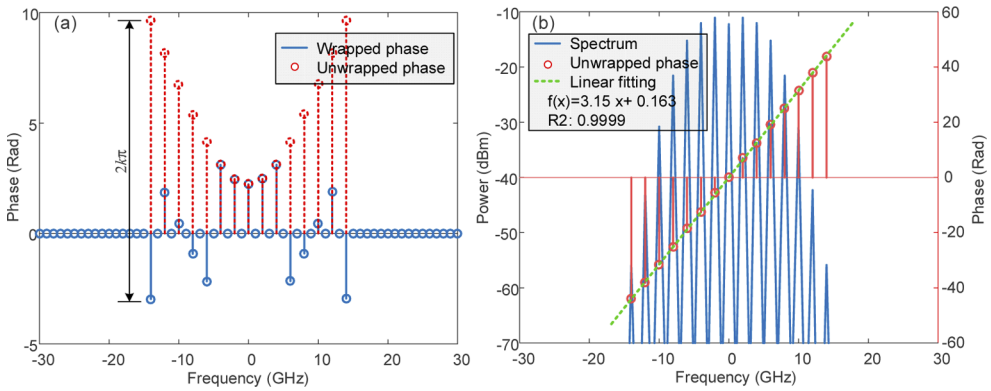

Fig. 3. (a) The phase function of the comb lines generated by the proposed dual-loop OEO before and after phase unwrap. The phase function after phase unwrapping is quadratic; (b) after phase compensation by a DCF with a dispersion coefficient of −890 ps/nm, the phase function of the comb lines becomes linear phase.

Optics EXPRESS

terms of the comb line by adding or subtracting an integer multiple of 2π, the phase function of the comb becomes approximately a quadratic function, as shown as the red dotted line in Fig. 3(a). We know that a dispersive element with linear dispersion has a quadratic phase response, which can be used to compensate for the phase function, to make it from quadratic to linear. Figure 3(b) shows the amplitudes and phases of the comb lines after the optical comb propagates through a DCF with a dispersion coefficient of −890 ps/nm. The phase function is now linear. Through linear fitting, we have a coefficient of determination (R^2) of 0.9999, confirming good linearity after phase compensation, as shown in Fig. 3(b). Thus, a transform-limited pulse train can be generated by applying the comb lines to a PD.

3. Results

3.1. Simulation

In the proposed system, the oscillation frequency, the power of the microwave signal applied to the modulators and the dispersion coefficient of the DCF are three parameters that would affect the generation of the ultra-short pulse train. In the following, a numerical simulation is performed to investigate the adjustments of the three parameters on the generated pulse train.

First, we set the amplitude of the microwave signal applied to the MZM to be fixed at $1.6V_\pi/\pi$ and tune the amplitude of the microwave signal applied to the PM from 0 to $8V_\pi/\pi$, the results are shown in Fig. 4. As can be seen, when the amplitude of the microwave signal applied to the PM is increased, the number of the optical comb lines of the generated optical comb is also increased, as shown in Fig. 4(a). The corresponding transform-limited temporal waveforms are shown in Fig. 4(b). It can be seen when the amplitude of the microwave signal applied to the PM is increased, an optical comb with more comb lines is generated, which leads to a pulse train with a narrower pulse width. Figure 4(c) and (d) illustrates the effect of the value of chromatic dispersion on the generated pulse train. The OEO is assumed to have an oscillation frequency of 6.0 GHz and a constant oscillation power. With the dispersion coefficient of the DCF at three different values of −173, 0, and 433 ps/nm, a pulse train with three different pulse widths are generated. Among the three, the value of the dispersion coefficient of 433 ps/nm leads to a pulse train with the smallest pulse width of 7.3 ps. When the value of the dispersion coefficient is 0 ps/nm, or equivalently no DCF, is employed, the pulse width is very wide due to the quadratic phase function of the optical comb. When the value of dispersion coefficient is −173 nm/ps, the pulse width is again compressed to 7.5 ps. The simulation results agree well with our theoretical study that the pulse width is jointly determined by the modulation frequency, the modulation signal powers and the value of the chromatic dispersion.

3.2. Experimental results

An experiment is then performed based on the system shown in Fig. 1 to evaluate the operation of the OEO for pulse train generation. An optical carrier at 1548.46 nm with an optical power of 12 dBm is generated by the LD (OVLINK MT-2831-4.3 L13) which is sent to the PM via PC1. The PM (H74M-5208-J049) has a bandwidth of 10 GHz. The phase modulated signal is sent to the MZM via SMF1 and the ODL. The MZM (SN-334971D) has a bandwidth of 10 GHz. The signal at the output of the MZM is split into two parts, with one being sent to PD2 through SMF2 and the EDFA. The lengths of the two SMFs, SMF1 and SMF2, are 2.07 and 1.04 km, respectively. An EBPF (AV11616) with a central frequency of 2.023 GHz and a 3-dB bandwidth of 100 MHz is connected to the output of PD2 (New Focus 1014, bandwidth 45 GHz) for frequency selection. EA1, consisting of three amplifies (DBPA2500022200A, OA4SMM4, EVK-RF-A-40S-M), is connected to the output of the EBPF to make the gain of the two loops greater than the loss. The signal at the output of EA1 is split into two parts, with one being sent to the MZM to close the short OEO loop and the other, after frequency doubling by the frequency multiplier and further

Optics EXPRESS

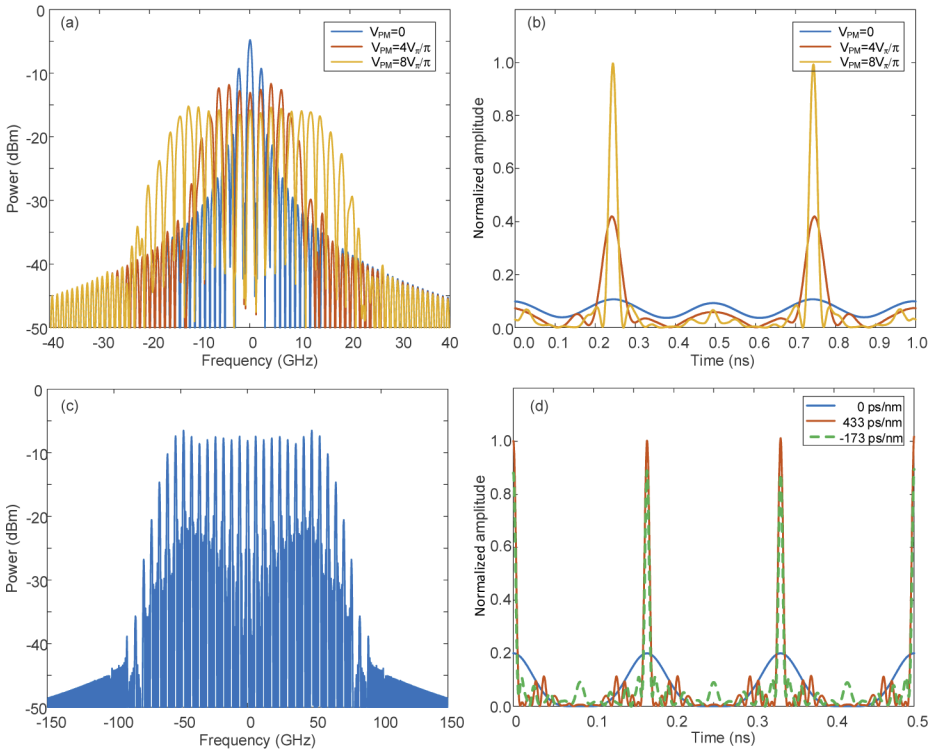

Fig. 4. (a) Simulated optical spectra at the output of the MZM when the amplitude of the modulation signal applied to the PM is changed while the amplitude of the modulation signal applied to the MZM is fixed at $1.6V_\pi/\pi$. The OEO oscillation frequency is at 2 GHz. (b) The corresponding output pulse trains when the dispersion coefficient of the DCF is −890 ps/nm. (c) Simulated optical spectra when the amplitudes of the microwave modulation signals applied to the PM and MZM are $10V_\pi/\pi$ and $1.6V_\pi/\pi$, respectively. The oscillation frequency is at 6 GHz. (d) The corresponding output pulse trains when the dispersion coefficients of the DCF are 0, 433, and −173 ps/nm.

amplified by EA2, is applied to the PM to close the long OEO loop. The second part of the signal at the output of the MZM is sent to the DCF and applied to PD1 (New Focus 1014, bandwidth 45 GHz). The DCF has a dispersion coefficient of −995.6 ps/nm. The generated pulse train is analyzed by an ESA (Keysight N9020B) and an OSC (Lab-Master 10-36Zi). The OSC has a sampling rate of 80 GSa/s and a bandwidth of 36 GHz.

As the OEO loops are closed, a microwave pulse train is generated at the output of PD1. Figure 5 shows measured spectrum and temporal waveform of the pulse train. The pulse train has a repetition frequency of 2.023 GHz, which is the oscillating frequency of the OEO determined by the EBPF. Due to the cascaded modulations, a frequency comb with more than ten comb lines is generated. The temporal waveform shows that the pulse width is as small as 40 ps, which is only three times the sampling interval of the OSC. Our system can generate shorter pulses at a higher repetition rate of over 10 GHz by increasing the fundamental oscillating frequency of the OEO. However, a sampling system with a higher sampling rate and a larger bandwidth should be used. In Fig. 5(b), a simulated waveform is also shown, which is calculated by using the same dispersion coefficient of −995.6 ps/nm of the DCF. The dispersion coefficient is an optimal value according to our simulation and the dashed line shows the simulation results. Good agreement between the simulated and experimental waveforms is achieved.

Optics EXPRESS

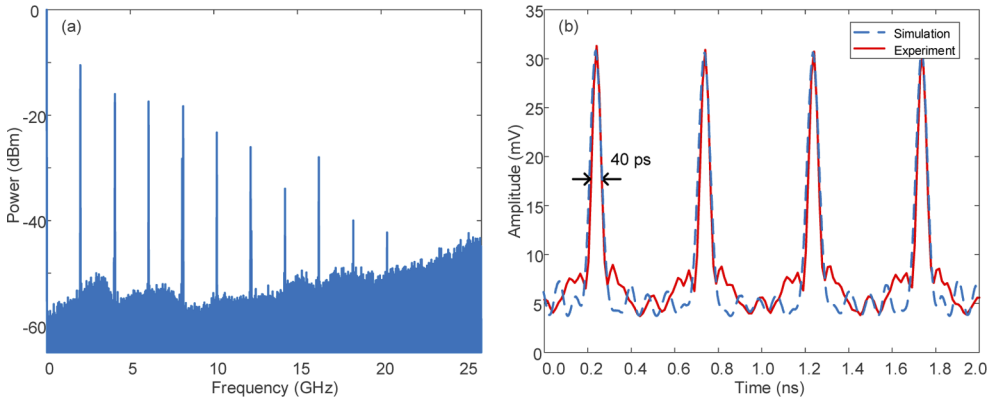

Fig. 5. (a) Electrical spectrum and (b) temporal waveform of the generated pulse train. In (b), a simulated waveform is also included for comparison.

It should be noted that the pulse width can be further reduced if an optical comb with broader bandwidth can be generated, which can be achieved by using more cascaded modulators and modulators with higher modulation indices. The use of fiber nonlinearities can also increase the number of comb lines, to reduce the pulse width.

The time jitter of the pulse train cannot be directly detected in the time domain due to the limited sampling rate of the OSC. To determine the time jitter of the pulse train, we measure the phase noise of the fundamental frequency generated by the OEO. As shown in Fig. 6, the phase noise for the generated microwave carrier at 2 GHz is −118 dBc/Hz at an offset frequency of 10 kHz. The sidemodes are lower than −88.64 dBc/Hz, with the first sidemode located at an offset frequency of 182 kHz from the microwave carrier, corresponding to the mode spacing of the short loop. We calculate the phase noise power within different offset frequency ranges using Eq. (8), which are then converted to time jitter using Eq. (7), as shown in Fig. 6. The total time jitter of the pulse train is calculated by the total phase noise power using Eq. (8), which is 391.2

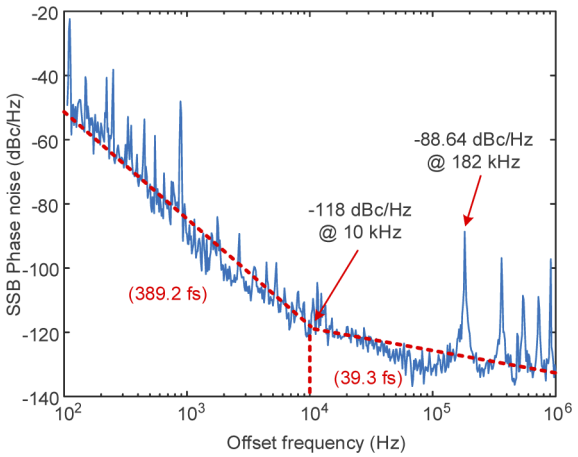

Fig. 6. The measured SSB phase noise of the generated microwave carrier at 2 GHz. The phase noise from 100 Hz to 10 kHz and from 10 kHz to 1 MHz correspond to a time jitter of 389.2 and 39.3 fs, respectively. The total phase noise is converted to a time jitter of 391.2 fs (red dotted lines).

Optics EXPRESS

fs. Since a pulse train is launched into the PD rather than a single tone signal, the nonlinearity in the PD may introduce additive phase noise to its output due to the amplitude to phase noise conversion. The actual time jitter of the optical pulse train may be lower than measured. The phase noise at low offset frequency band below 1 kHz is the main contributor to the time jitter, which accounts for 389.2 fs. Since the OEO does not include an active loop to stabilize the operation, the operation is strongly affected by temperature drift and mechanical vibrations from the environment, thus resulting in strong phase noise at low offset frequencies [21,31]. If active feedback control is incorporated in the OEO loop, the phase noises at low offset frequencies can be effectively suppressed, thereby drastically reducing the time jitter. In addition, low-noise PD and amplifiers should also incorporated to reduce the system noise. We estimate that the time jitter can be reduced to be less than 18 fs using the phase noise measurement of a similar OEO with improved phase noise performance [4,24,26,27].

4. Conclusion

In conclusion, we have proposed and experimentally demonstrated the generation of an ultra-short pulse train with low time jitter based on a dual-loop OEO incorporating two cascaded PM and MZM and a DCF. Thanks to the dual loops, the effective FSR was increased which helped the mode selection for single-frequency oscillation. The cascaded PM and MZM were also used for the generation of an optical comb with more comb lines. Our analysis showed that the comb has a quadratic phase function, which was converted to a linear phase function by a DCF, pulse compression was then achieved. The proposed approach was evaluated experimentally. A pulse train with a repetition rate of 2.023 GHz and a pulse width of 40 ps was generated. The SSB phase noise of the fundamental frequency was measured to be −118 dBc/Hz at 10-kHz offset frequency, corresponding to a time jitter of 391.2 fs. Since the phase noise of an OEO at low offset frequencies can be dramatically decreased if an active stabilization loop is incorporated, we estimate that the time jitter can be reduced to be as low as 18 fs. Additionally, the pulse width can be reduced by generating an optical comb with more comb lines using more cascaded modulators and modulators with higher modulation indices. The use of fiber nonlinear effects can also be considered for increasing the number of comb lines.

Funding. Guangdong Province Key Field R&D Program Project (2020B0101110002); National Natural Science Foundation of China (61860206002, 61905095).

Disclosures. The authors declare no conflicts of interest.

Data availability. Data underlying the results presented in this paper are not publicly available at this time but may be obtained from the authors upon reasonable request.

References

1. B. Jamali, "Integrated Millimeter-Wave and Sub-Terahertz Pulse Receivers for Wireless Time Transfer and Broadband Sensing," (Rice University, 2019).
2. J. Yao, "Microwave photonics," J. Lightwave Technol. **27**(3), 314–335 (2009).
3. Y. Na, C.-G. Jeon, C. Ahn, M. Hyun, D. Kwon, J. Shin, and J. Kim, "Ultrafast, sub-nanometre-precision and multifunctional time-of-flight detection," Nat. Photonics **14**(6), 355–360 (2020).
4. J. Lasri, P. Devgan, R. Tang, and P. Kumar, "Ultralow timing jitter 40-Gb/s clock recovery using a self-starting optoelectronic oscillator," IEEE Photonics Technol. Lett. **16**(1), 263–265 (2004).
5. J. Kim and Y. Song, "Ultralow-noise mode-locked fiber lasers and frequency combs: principles, status, and applications," Adv. Opt. Photonics **8**(3), 465–540 (2016).
6. X. S. Yao, L. Davis, and L. Maleki, "Coupled optoelectronic oscillators for generating both RF signal and optical pulses," J. Lightwave Technol. **18**(1), 73–78 (2000).
7. E. Salik, N. Yu, and L. Maleki, "An ultralow phase noise coupled optoelectronic oscillator," IEEE Photonics Technol. Lett. **19**(6), 444–446 (2007).
8. N. Yokota and H. Yasaka, "Cascaded SSB comb generation using injection-locked seed lasers," Opt. Lett. **46**(4), 769–772 (2021).
9. P. Zhou, F. Zhang, B. Gao, and S. Pan, "Optical pulse generation by an optoelectronic oscillator with optically injected semiconductor laser," IEEE Photonics Technol. Lett. **28**(17), 1827–1830 (2016).

Optics EXPRESS

10. H. Murata, A. Morimoto, T. Kobayashi, and S. Yamamoto, "Optical pulse generation by electrooptic-modulation method and its application to integrated ultrashort pulse generators," IEEE J. Sel. Top. Quantum Electron. **6**(6), 1325–1331 (2000).
11. Y. He, Y. Jiang, Y. Zi, G. Bai, J. Tian, Y. Xia, X. Zhang, R. Dong, and H. Luo, "Photonic microwave waveforms generation based on two cascaded single-drive Mach-Zehnder modulators," Opt. Express **26**(6), 7829–7841 (2018).
12. C. He, S. Pan, R. Guo, Y. Zhao, and M. Pan, "Ultraflat optical frequency comb generated based on cascaded polarization modulators," Opt. Lett. **37**(18), 3834–3836 (2012).
13. T. Sakamoto, T. Kawanishi, and M. Tsuchiya, "10 GHz, 2.4 ps pulse generation using a single-stage dual-drive Mach-Zehnder modulator," Opt. Lett. **33**(8), 890–892 (2008).
14. T. Yang, J. Dong, S. Liao, D. Huang, and X. Zhang, "Comparison analysis of optical frequency comb generation with nonlinear effects in highly nonlinear fibers," Opt. Express **21**(7), 8508–8520 (2013).
15. H. Nakatsuka, D. Grischkowsky, and A. Balant, "Nonlinear picosecond-pulse propagation through optical fibers with positive group velocity dispersion," Phys. Rev. Lett. **47**(13), 910–913 (1981).
16. I. Morohashi, T. Sakamoto, H. Sotobayashi, T. Kawanishi, and I. Hosako, "Broadband wavelength-tunable ultrashort pulse source using a Mach–Zehnder modulator and dispersion-flattened dispersion-decreasing fiber," Opt. Lett. **34**(15), 2297–2299 (2009).
17. V. Ataie, E. Myslivets, B. P.-P. Kuo, N. Alic, and S. Radic, "Spectrally equalized frequency comb generation in multistage parametric mixer with nonlinear pulse shaping," J. Lightwave Technol. **32**(4), 840–846 (2014).
18. M. A. Soto, M. Alem, M. A. Shoaie, A. Vedadi, C.-S. Brès, L. Thévenaz, and T. Schneider, "Optical sinc-shaped Nyquist pulses of exceptional quality," Nat. Commun. **4**(1), 1–11 (2013).
19. X. S. Yao and L. Maleki, "Multiloop optoelectronic oscillator," IEEE J. Quantum Electron. **36**(1), 79–84 (2000).
20. W. Li and J. Yao, "A wideband frequency tunable optoelectronic oscillator incorporating a tunable microwave photonic filter based on phase-modulation to intensity-modulation conversion using a phase-shifted fiber Bragg grating," IEEE Trans. Microwave Theory Tech. **60**(6), 1735–1742 (2012).
21. J. Zhang and J. Yao, "Parity-time–symmetric optoelectronic oscillator," Sci. Adv. **4**(6), eaar6782 (2018).
22. J. Zhang, L. Li, G. Wang, X. Feng, B.-O. Guan, and J. Yao, "Parity-time symmetry in wavelength space within a single spatial resonator," Nat. Commun. **11**(1), 3217 (2020).
23. A. O. Wiberg, L. Liu, Z. Tong, E. Myslivets, V. Ataie, B. P.-P. Kuo, N. Alic, and S. Radic, "Photonic preprocessor for analog-to-digital-converter using a cavity-less pulse source," Opt. Express **20**(26), B419–B427 (2012).
24. J. Dai, X. Xu, Z. Wu, Y. Dai, F. Yin, Y. Zhou, J. Li, and K. Xu, "Self-oscillating optical frequency comb generator based on an optoelectronic oscillator employing cascaded modulators," Opt. Express **23**(23), 30014–30019 (2015).
25. B. Brannon, "Sampled systems and the effects of clock phase noise and jitter," Analog Devices App. Note **AN-756**, 1–11 (2004).
26. L. Zhang, A. Poddar, U. Rohde, and A. S. Daryoush, "Phase noise reduction and spurious suppression in oscillators utilizing self-injection loops," in *2014 IEEE Radio and Wireless Symposium (RWS)*, (IEEE, 2014), 187–189.
27. A. Hati, C. W. Nelson, J. Taylor, N. Ashby, and D. Howe, "Cancellation of vibration-induced phase noise in optical fibers," IEEE Photonics Technol. Lett. **20**(22), 1842–1844 (2008).
28. W. Zhou and G. Blasche, "Injection-locked dual opto-electronic oscillator with ultra-low phase noise and ultra-low spurious level," IEEE Trans. Microwave Theory Tech. **53**(3), 929–933 (2005).
29. X. Zhang, D. Peng, Y. Ma, B. Wang, M. Wang, Z. Li, Z. Zhang, S. Zhang, H. Li, and Y. Liu, "Broadband high-resolution microwave frequency measurement based on photonic undersampling via using three cavity-less optical pulse sources with coprime repetition rates," Appl. Opt. **59**(27), 8056–8065 (2020).
30. S. Kumar and M. J. Deen, *Fiber optic communications: fundamentals and applications* (John Wiley & Sons, 2014).
31. J. Hong, S. X. Yao, Z. L. Li, J. X. Huang, X. W. Fang, and J. Guo, "Fiber-length-dependence phase noise of injection-locked optoelectronic oscillator," Microw. Opt. Technol. Lett. **55**(11), 2568–2571 (2013).